Remote Sensing and Geographic Information Systems for Design and Operation of Water Resources Systems (Proceedings of Rabat Symposium S3, April 1997). IAHS Publ. no. 242, 1997

Advanced analysis of snow cover based on satellite remote sensing for the assessment of water resources

C. EHRLER, K. SEIDEL & J. MARTINEC

Communication Technology Laboratory ETHZ — Image Science Division, Gloriastrasse 35, CH-8092 Zürich, Switzerland

Abstract A method is presented to extrapolate the snow cover from the visible areas of an elevation zone to areas obscured by clouds. The satellite images are combined with so called Snow Cover Units (SCU). These are obtained by overlaying features such as ground properties, regions of similar snow accumulation, elevation, aspect and slope. The effect of the above-mentioned factors on the seasonal decrease of snow cover is demonstrated in three Alpine basins. The method enables partially cloud covered scenes to be used for high resolution snow cover mapping from Landsat-TM and SPOT-XS data.

INTRODUCTION

Monitoring of the seasonal snow cover by satellites is an important tool for snowmelt runoff computation and for the evaluation of snow reserves in mountain basins. As a new application, it is increasingly used to study the effect of a changed climate on snow cover and runoff. The main obstacle concerning snow cover mapping by optical sensors is a frequent interference of clouds. In order to derive the seasonal decrease of the areal extent of snow covered areas, at least four satellite images are needed during each snowmelt season. The images influenced by snowfalls preceding a satellite overflight must be discarded. Consequently, satellites with a high spatial resolution but a low overflight frequency, like Landsat, have little chance to meet these requirements each year. The presented method makes a realistic extrapolation of the snow cover from visible parts of an elevation zone to parts obscured by clouds possible, so that precision snow cover mapping can be carried out from partially cloud-covered scenes.

ALPINE BASINS SELECTED FOR THE STUDY

As shown in Fig. 1, the three selected test basins are located in the central Swiss Alps. The basin of the Upper Rhine at Felsberg (3250 km^2, 560-3614 m a.s.l., glacier covered area 64 km^2) has been divided into five elevation zones. This basin has a considerable history of snow cover mapping by Landsat, SPOT and NOAA/AVHRR satellites for snowmelt runoff simulations (Baumgartner, 1987; Baumgartner *et al.*, 1987), evaluation of snow reserves (Martinec *et al.*, 1991) and, in sub-basins, for operational runoff forecasts (Brüsch, 1995; Seidel *et al.*, 1995). The average runoff (1961-1980) is 115 m^3 s^{-1} which corresponds to a yearly runoff depth of 111.6 cm.

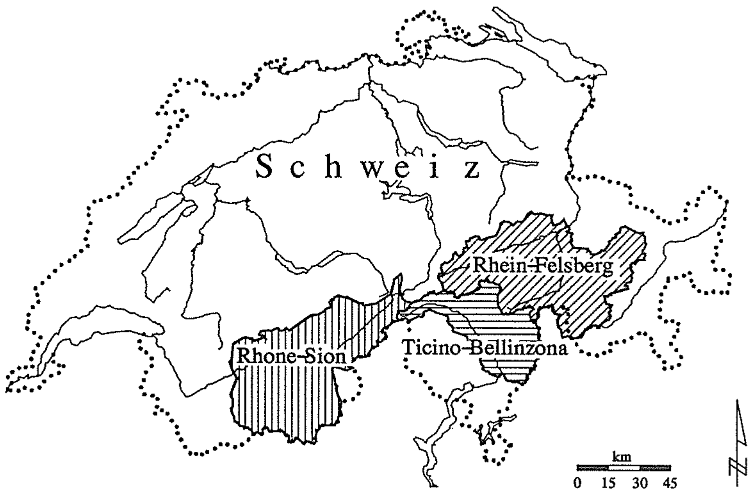

Fig. 1 Location of the test basins in the central Swiss Alps.

The basin of the Rhône at Sion (3371 km^2, 491-4634 m a.s.l.) is characterized by a relatively high glacier covered area of 580 km^2. It has been divided into seven elevation zones. The average runoff (1961-1980) is 112 $m^3 s^{-1}$, corresponding to a yearly runoff depth of 104.8 cm.

The south facing basin of the River Ticino at Bellinzona has an area of 1515 km^2, an elevation range of 220-3402 m a.s.l. and glacier covered area of 8.1 km^2. It has been divided into five elevation zones. The average runoff (1961-1980) is 64.3 $m^3 s^{-1}$, which corresponds to a yearly runoff depth of 133.8 cm.

SATELLITE SNOW COVER MAPPING

High resolution satellite data, such as Landsat-TM and SPOT-XS, allow a detailed analysis of the changing snow cover distribution during the snowmelt season (1 April-30 September).

For the above-mentioned test basins all available satellite recordings have been geocoded and even georeferenced in case of large relief distortions using a Digital Elevation Model. The multispectral data have been thematically interpreted with respect to snow, transition zone and snow-free (= aper) and additionally with respect to ice for the heavily glacierized basin of Rhône-Sion. The differences in illumination due to topography have been taken into account for the classification in order to guarantee a correct interpretation in shadowed areas as well as on weakly illuminated slopes (Ehrler & Seidel, 1995).

For this investigation only recordings have been used which were not influenced by snowfalls preceding the satellite overflight.

The spatial snow distribution patterns derived from the different satellite images were transferred into a geographic information system (GIS) in order to allow detailed quantitative statistical analyses with regard to various aspects of the Snow Cover Units (SCU). The SCU are defined as assemblies of patches with similar snow

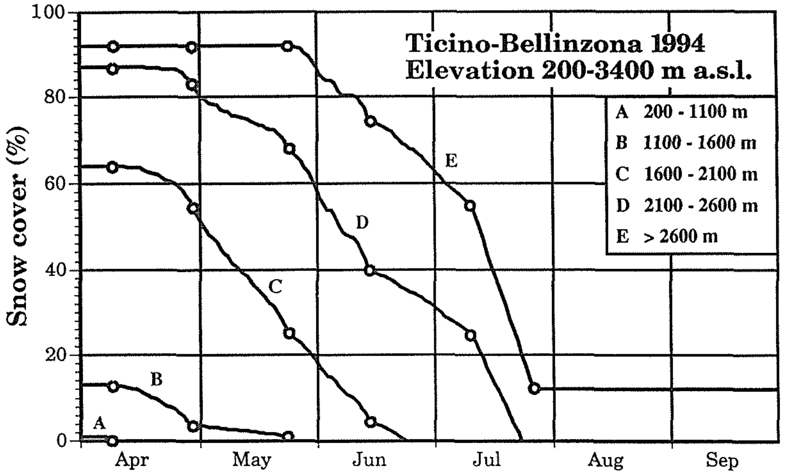

Fig. 2 Example of depletion curves of the snow cover for the elevation zones A, B, C, D, E, of the Ticino basin at Bellinzona 1994.

cover. They are obtained by superimposing bio-physical features (ground properties), topographic properties (elevation, aspect, slope) and affiliation to climatic regions (regions of snow accumulation).

VARIATIONS OF THE SNOW COVER DECLINE WITHIN AN ELEVATION ZONE

In mountain basins, the depletion curves of the snow cover decline earlier in the lower elevation zones than in the higher zones as illustrated in Fig. 2 for the basin of Ticino at Bellinzona. This is caused by snow accumulation increasing with altitude and snowmelt rates simultaneously decreasing with altitude. In addition, summer precipitation is more likely to occur as snow in the higher areas, slowing down the decline of the depletion curves. However, as has been pointed out earlier (Seidel *et al.*, 1983), the snow cover may vary in certain areas of an elevation zone. Consequently it is not possible to extrapolate the percentage of the snow covered area from the visible parts of a zone to parts obscured by clouds without taking these deviations into account.

The differences in snow cover depletion curves are caused by different initial accumulation including redeposition of snow in each partial area and by different melt rates.

As illustrated in Fig. 3 for the Rhône-Sion basin, the summer coverage is highest with the snow cover superimposed on glaciers, followed by permafrost as underlying ground. Evidently reduced melt rates result from this configuration.

Since the SCUs depend upon ground properties they vary in size. In order to eliminate the influence of differently sized SCUs, an unweighted average has been used as reference to determine the deviations. This leads to smaller deviations than

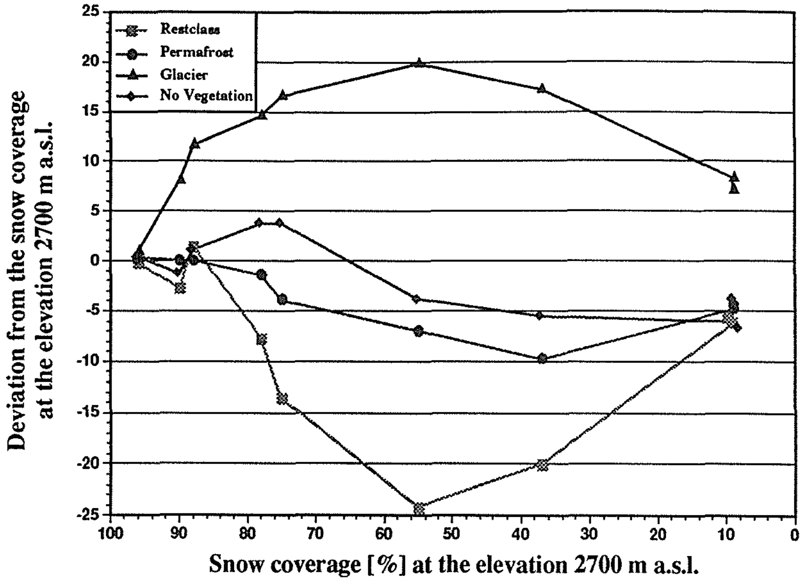

Fig. 3 Effect of ground properties: Deviations of the snow cover from the average interpolated altitude to 2700 m a.s.l. in partial areas with different ground properties, basin Rhone at Sion, 1985.

those shown in Figs 3, 5, 6 and 7, but the relative position of the lines is not changed. Similar results are obtained in the other two test basins as documented in Table 1.

Figure 4 shows a subdivision of the test basins into typical regions with a different snow accumulation. As seen in Fig. 5, the snow cover is higher in the

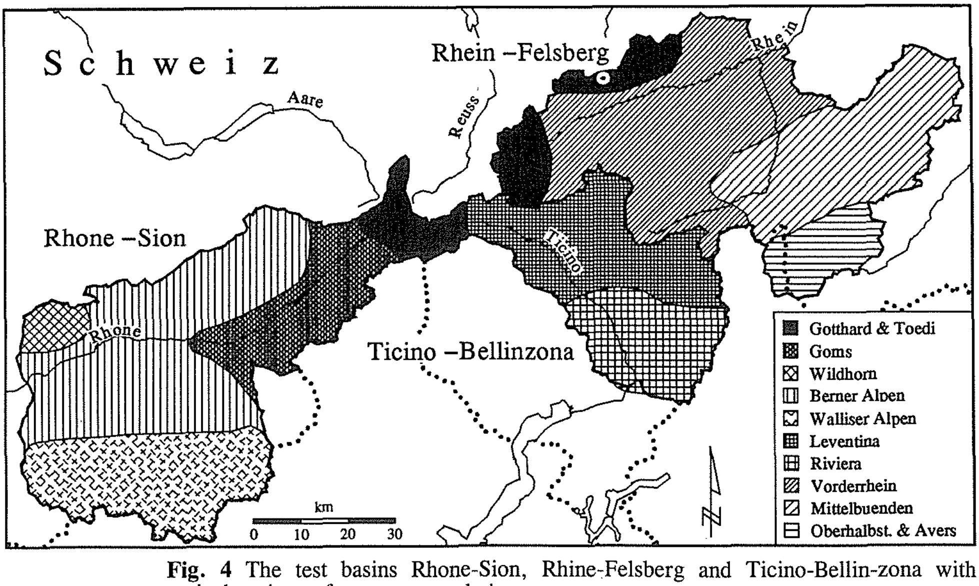

Fig. 4 The test basins Rhone-Sion, Rhine-Felsberg and Ticino-Bellin-zona with typical regions of snow accumulation.

Table 1 Deviations of the snow coverage from the average of all snow cover units (SCU) for various types of ground, typical regions of snow accumulation, aspects and slopes, for elevation zone D (2100-2600 m a.s.l.).

Basin	Rhine-Felsberg	Rhône-Sion	Ticino-Bellinzona
Years	1982 1985 1990 1992 1993 1994	1985	1994
Number of images (10%≤S≤90%)	11	5	6
	deviations from unweighted average (%) of S		
Glacier[a]	+20[b]	+9	+12[b]
Permafrost probable[a]	0	-3	-1
without vegetation[a]	-3	-1	-3
Rest-class[a]	*-12*	*-5*	*-8*
Range for Ground Properties[a]	**32**	**14**	**20**
Gotthard region	+12	+16	+15
Vorderrhein, Wildhorn region	-1	+15	+2
Middle Grisons/Goms/Riviera	*-6*	+1	*-18*
Oberhalbstein/Bernese Alps/-	*-6*	-8	-
-/Wallis Alps/-	-	*-25*	-
Range for typical regions of snow accumulation	**18**	**41**	**33**
North	+5	+5	+9
North-East	+7	+5	+6
East	+8	+4	+4
South-East	+4	+3	-3
South	-6	-8	-9
South-West	*-10*	*-10*	*-10*
West	*-10*	-8	-5
North-West	-2	-2	+3
Range for Exposition	**18**	**15**	**19**
<8°	+13	+9	+2
8°-18.9°	+10	+7	+5
19°-27.9°	+5	+3	+4
28°-35.9°	-4	-4	0
36°	*-14*	*-16*	*-11*
Range for Slopes	**27**	**25**	**16**

a. all ground classes interpolated to 2700 m a.s.l.
b. inclusive exposed glacier ice

Gotthard region than in the east due to a higher initial accumulation of snow. In the other two test basins, the highest accumulation of snow can also be found in the Gotthard region. The effect of aspect on snow cover in the Rhine-Felsberg basin is illustrated in Fig. 6. The snow cover is higher than the average in the northeast

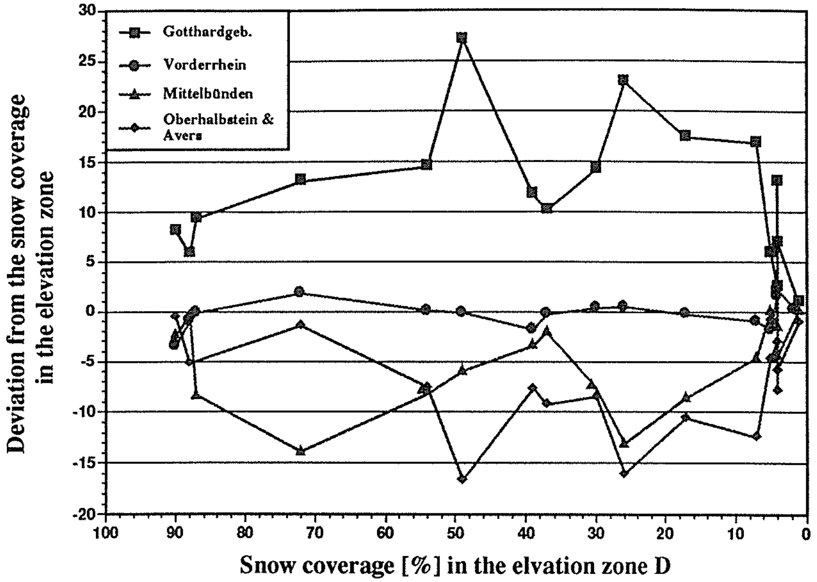

Fig. 5 Effect of regional variability: Deviations of snow cover from the average of the elevation zone D in the respective regions, basin of Rhine-Felsberg, compiled from snow-cover maps within six years.

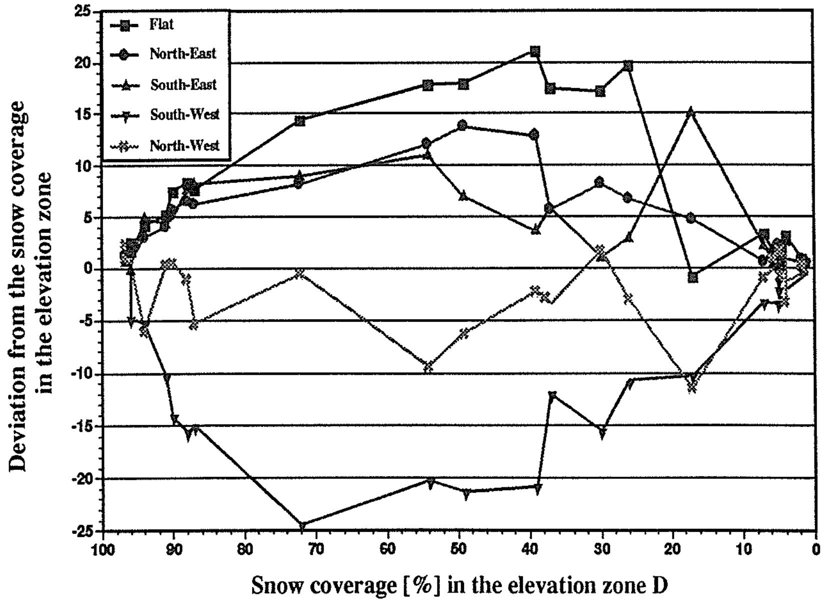

Fig. 6 Effect of aspect: Deviations of snow cover from the average of the elevation zone D in the respective regions, basin of Rhine-Felsberg, compiled from snow-cover maps within six years.

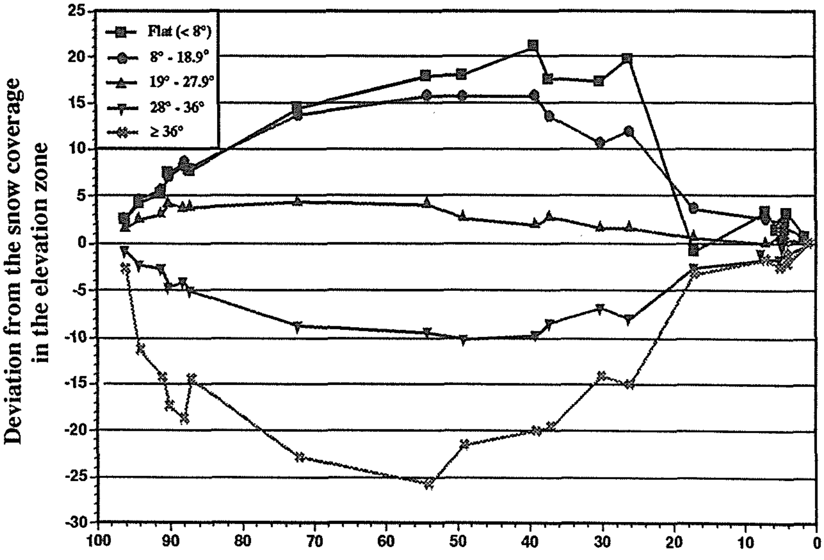

Fig. 7 Effect of slope: Deviation of snow cover from the average of the elevation zone D in the respective regions, basin of Rhine-Felsberg, compiled from snow-cover maps within six years.

aspect and lower in the southwest aspect. In addition to solar radiation, the initial pattern of snow accumulation may have altered influenced by the prevailing winds. Finally, Fig. 7 shows the effect of slope. In flat areas (actually an assembly of area units with a slope <8°), the snow cover is higher than the average value for the examined zone. In steep areas it is lower. Evidently snow is preferably deposited on small slopes while there is less snow on steep parts and rocky ridges.

Results for all test basins in the elevation zone D are listed in Table 1. With the exception of typical regions of snow accumulation, partial areas are assembled from areal units (SCU) of the same category. Results from the basin Rhine-Felsberg compiled from six years also show that the patterns of snow accumulation and ablation are repeated year after year, with only sporadic exceptions concerning the regional distribution of snow.

Table 2 Accuracy of snow cover mapping from partially cloud-free images extrapolated with Snow Cover Units (SCU). Extrapolation errors (EE) from results for cloud-free images with snow coverage between 10% and 90%.

Cloud coverage	10%	20%	30%	40%	50%	60%	70%
Number of samples	56	52	40	34	10	17	13
Average EE	-0.89	-1.54	-2.35	-3.24	-6.40	-3.94	-6.31
Maximum negative EE	-3	-5	-7	-9	-10	-13	-13
Maximum positive EE	2	3	3	3	(-2)[a]	3	3
Standard deviation of the EE	1.07	1.85	2.65	3.22	2.59	4.80	5.01

a. no positive EE

EXTRAPOLATION OF THE SNOW COVER TO CLOUD-OBSCURED AREAS

As has been illustrated in Fig. 2, the gradual decrease of the areal extent of the seasonal snow cover differs in the respective elevation zones. The detailed study outlined in the previous sections reveals that differences occur also within an elevation zone, due to the effect of ground properties, regional variations of snow accumulation, aspect and slope.

In order to evaluate the achievable accuracy of snow cover from images partially covered with clouds, snow covered areas obtained from cloud-free scenes were compared with results from the same scenes artificially obscured by various percentages of cloud cover, with the refined extrapolation using the snow cover units (SCU).

Data listed in Table 2 summarize the extrapolation errors (EE) as differences of the correct snow cover compared with the extrapolated values. It is shown that if e.g. 20% of a zone is obscured by clouds, the snow cover can be evaluated within 5% of the "cloud-free" percentage, considering extreme errors which occurred in 52 samples.

Even if more than the half of a zone is covered with clouds, a realistic snow cover mapping still appears to be feasible, although this result is based on a smaller number of samples.

CONCLUSIONS

With the use of the Snow Cover Units (SCU) incorporated in a geographic information system (GIS), it is possible to differentiate between the snow cover depletion patterns in each elevation zone. This procedure enables a realistic extrapolation of snow cover to be carried out in scenes partially obscured by clouds. Consequently the frequency of snow cover mapping by high resolution satellites like Landsat-TM and SPOT-XS can be significantly improved even in unfavourable years, as required for snowmelt runoff forecasts as well as for evaluations of the climate change effect on snow reserves and runoff.

Acknowledgement The authors thank Dr Felix Keller (ETH-VAW Zürich) for providing data on permafrost.

REFERENCES

Baumgartner, M. F. (1987) Schneeschmelz-Abflusssimulationen basierend auf Schneeflächenbestimmungen mit digitalen Landsat-MSS- und NOAA/AVHRR-Daten (Snowmelt runoff simulations based on snow cover mapping by digital Landsat-MSS and NOAA/AVHRR data) (in German). *Remote Sensing Series* **11**, Univ. of Zurich, Dept of Geography, Zurich, Switzerland.

Baumgartner, M. F., Seidel, K. & Martinec, J. (1987) Towards snowmelt runoff forecast based on multisensor remote-sensing information. *IEEE Trans. on Geoscience and Remote Sensing* **GE-25**, 746–750.

Brüsch, W. (1995) SRM-ETH: Das Snowmelt Runoff Model zur Erstellung von Tages- und Saisonabflussprognosen für Wasserkraftwerke (The snowmelt runoff model for day-to-day and seasonal runoff forecasts for hydroelectric plants) (in German). *Remote Sensing Series* **27**, Univ. of Zurich, Dept of Geography, Zurich, Switzerland.

Ehrler, C. & Seidel, K. (1995) Mutual effects of the climate change and the alpine snow cover and their influence on the runoff regime evaluated with the aid of satellite remote sensing. In: *IGARSS'95; Quantitative Remote Sensing for Science and Applications*, vol. 3 (ed. by T. I. Stein) (Proc. IGARSS'95, Florence, Italy), 1973–1975.

Martinec, J., Seidel, K., Burkart, U. & Baumann, R. (1991) Areal modelling of snow water equivalent based on remote sensing techniques. In: *Snow, Hydrology and Forests in High Alpine Areas* (ed by H. Bergmann, H. Lang, W. Frey, D. Issler & B. Salm) (Proc. Vienna Symp., August 1991), 121–129. IAHS Publ. no. 205.

Seidel, K., Ade, F. & Lichtenegger, J. (1983). Augmenting LANDSAT MSS data with topographic information for enhanced registration and classification. *IEEE Trans. on Geoscience and Remote Sensing* **GE-21**, 252–258.

Seidel, K., Brüsch, W., Steinmeier, C., Martinec, J. & Wiedemeier, J. (1995) Real time runoff forecasts for two hydroelectric stations based on satellite snow cover monitoring. In: *Sensors and Environmental Applications of Remote Sensing* (ed. by J. Askne) (Proc. 14th EARSeL Symp. 1994 in Göteborg, Sweden), 253–258. A. A. Balkema Rotterdam/Brookfield.